INTECH
open science | open minds

OPEN ACCESS
ARTICLE

International Journal of Advanced Robotic Systems

Closed-Loop Behavior of an Autonomous Helicopter Equipped with a Robotic Arm for Aerial Manipulation Tasks

Regular Paper

Konstantin Kondak[1], Kai Krieger[1], Alin Albu-Schaeffer[1], Marc Schwarzbach[1], Maximilian Laiacker[1], Ivan Maza[2,*], Angel Rodriguez-Castano[2] and Anibal Ollero[2]

1 Institute of Robotics and Mechatronics, DLR (German Aerospace Center), Oberpfaffenhoffen-Wessling, Germany
2 Robotics, Vision and Control Group, Universidad de Sevilla, Seville, Spain
* Corresponding author E-mail: imaza@us.es

Received 3 Jul 2012; Accepted 24 Sep 2012

DOI: 10.5772/53754

Abstract This paper is devoted to the control of aerial robots interacting physically with objects in the environment and with other aerial robots. The paper presents a controller for the particular case of a small-scaled autonomous helicopter equipped with a robotic arm for aerial manipulation. Two types of influences are imposed on the helicopter from a manipulator: coherent and non-coherent influence. In the former case, the forces and torques imposed on the helicopter by the manipulator change with frequencies close to those of the helicopter movement. The paper shows that even small interaction forces imposed on the fuselage periodically in proper phase could yield to low frequency instabilities and oscillations, so-called phase circles.

Keywords Aerial Manipulation, Aerial Robots

1. Introduction

Aerial manipulators are a particular class of Unmanned Aerial Systems (UAS) physically interacting with the environment. Other classes include aerial slung load transportation and deployment as in Bernard et al. (2011), perching for refuelling and battery recharging, remote inspection by contact as in the European AIRobot (http://www.airobots.eu/) project and the cleaning of windows or walls by applying forces while maintaining flight stability that can be found for example in Albers et al. (2010).

Free flying robots with some manipulation capabilities have been proposed for space applications since the 1980s. These applications include inspection, assembly, capture, repair and maintenance capabilities in orbit. Unlike fixed-based robots, the base body of free flying robots is allowed to respond freely to dynamic reaction forces due to the motion of the arm or arms. In these systems there is a dynamic coupling between the motion of the arm (or arms) and the base. Also the joint control torques are limited due to actuator weight constraints in space.

The kinematics and dynamics of free-floating space manipulator systems were described 25 years ago using

the virtual manipulator approach in Vafa & Dubowsky (1987; 1990). In Umetani & Yoshida (1987), a generalized Jacobian matrix that reflects both momentum conservation laws and kinematic relations is used to study rigid space manipulators with revolute joints by assuming that no external forces are applied. This generalized Jacobian converges to the conventional Jacobian of the manipulator when the base is relatively massive. In Caccavale & Siciliano (2001), the generalized Jacobian is used to study the inverse kinematics. In Moosavian & Papadopoulos (1998), approaches for the kinematics modelling of a multibody space robotic system are presented. In Moosavian & Papadopoulos (2007), a review of dynamic modelling, planning and control problems for free flying robots in space is presented.

Recently, several researchers have been proposing unmanned aerial systems with grasping capabilities. In Pounds & Dollar (2010), a small RC helicopter with a gripper is able to grasp an object on the ground while in flight by means of a underactuated compliant gripper mounted ventrally between the aircraft's skids. In Pounds et al. (2011), the stability of the helicopter in contact with the object and/or the ground is studied. In particular, the longitudinal dynamics is studied and the payload effect is modelled by means of a pitch moment.

In Mellinger et al. (2010), grasping and cooperative transporting loads with quadrotors is presented. Furthermore, in Mellinger et al. (2011), several light-weight, low-complexity grippers that allow quadrotors to grasp and perch on branches or beams and pick up and transport payloads are presented. The inertial parameters of the grasped object are estimated and used to adapt the controller and improve performance during flight.

Reference Lindsey et al. (2011) presents structure construction experiments by means of indoor quadrotors with grippers.

In Korpela et al. (2012), a hybrid quadrotor-blimp prototype to test some aerial manipulation concepts is presented. In Orsag et al. (2012), the challenges in controlling a mobile manipulating UAV using a commercially available aircraft with three light-weight arms each with two degrees of freedom (DoF) is investigated.

Section 2 introduces general concepts related to aerial manipulation in the context of the European FP7 project ARCAS. The particular case of an autonomous helicopter equipped with a hand that can be used for general manipulation tasks is presented. Section 3 discusses control systems for aerial manipulation. In Section 4 the closed-loop behaviour is analysed and some simulations are presented. Section 5 closes the paper with the conclusions.

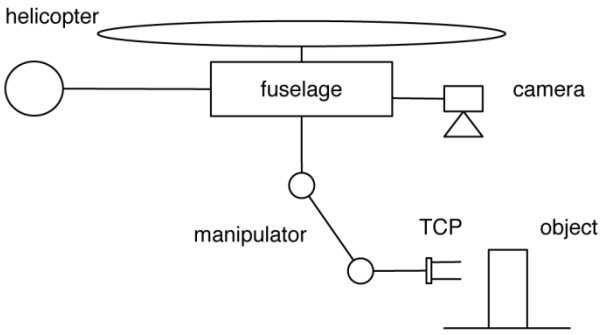

Figure 1. Scheme of the system for aerial manipulation based on an autonomous helicopter.

2. Aerial manipulation - the ARCAS project

In a broad sense, aerial manipulation involves a large number of functionalities from taking sole probes and picking up objects, to performing assembly operations involving force interactions with the objects.

The limitation in payloads and in general of take-off weight is a main concern and implies manipulators with reduced working space or even with less than six degrees of freedom (DoF). Therefore, it is desirable to increase the helicopter positioning precision in order to facilitate the manipulation task or even to realize some DoF of Tool Centre Point (TCP) of the manipulator by moving the helicopter fuselage.

Figure 1 shows an aerial manipulator system comprising a helicopter and a manipulator mounted on the fuselage. The task of this system is to fly close enough to the object to perform a manipulation task. The helicopter is equipped with a position sensor (e.g., GPS) and an orientation sensor (e.g., IMU) for estimation of the fuselage position and orientation in an inertial frame. The on-board perception system can be used for precise positioning and to track the position and orientation of the object with respect to the TCP.

As mentioned above, one of the main limitations in aerial manipulation is the payload of the Unmanned Aerial Vehicle (UAV). In order to overcome this limitation, the ARCAS project aims at the development and experimental validation of the first cooperative flying robot system for assembly and structure construction. In addition to the payload limitation, the adoption of several unmanned aerial aircraft instead of a single powerful one presents advantages such as enhanced manipulation capabilities, increased reliability and reduced costs.

In ARCAS both helicopters and quadrotor systems with arms, manipulation and perception devices are being developed.

Figure 2 shows the first helicopter-based set-up for experimenting on precision positioning helicopter

control. This set-up is composed of an electrical helicopter with the take-off weight of 15 kg and the rotor diameter of 2 m. The helicopter is equipped with a mechanical hand mounted on a cardan joint that compensates the roll and pitch angles of the fuselage. The cardan joint will be replaced by a manipulator with five DoF.

Figure 2. Experimental set-up for precision control with integrated vision system.

A perception system has been integrated on the helicopter for precise positioning, tracking and guidance of the assembly operations. Alternatively, in ARCAS, the environment perception system can be carried out by other UAS by implementing cooperative perception systems. The integration of the information from multiple aerial robots will also be used in range-only Simultaneous Localization and Mapping (SLAM) techniques.

ARCAS also includes the development of coordinated control of multiple cooperating aerial systems grasping the same object and cooperative planning for assembly, disassembly or inspection tasks by maintaining the safety in the simultaneous operation of multiple flying robots. The ARCAS architecture will integrate autonomous perception, planning and control with the intervention of human operators by using virtual reality haptics.

ARCAS experiments with autonomous helicopters as shown in Fig. 2 are being performed in an outdoor scenario in order to demonstrate advanced manipulation and assembly capabilities with integrated force/torque sensors. Moreover, indoor experiments are being performed with autonomous quadrotors and the VICON system for positioning to test basic manipulation and assembly functions with simple and light devices satisfying the payload constraints of the indoor quadrotors.

ARCAS is also targeting industrial inspection, maintenance and repair scenarios, as well as space applications with free-flying robots.

3. Control systems

Figure 3 shows a basic control scheme composed of an inner loop for orientation control, $\mathbf{R}_{ori}$, and an outer loop for position control, $\mathbf{R}_{pos}$. The output of the perception system - position of the object relative to the helicopter - is integrated at the input side of the outer loop. The performance of the whole system is given by the performance of the main controller. The combination of linear controller with non-linear dynamical and kinematical inversion blocks are used. More detail on the main controller can be found in Kondak et al. (2007).

Using this set-up in the flight experiments it was possible to validate that the grasping of a simple object is even possible without translational movement of TCP relative to the helicopter fuselage.

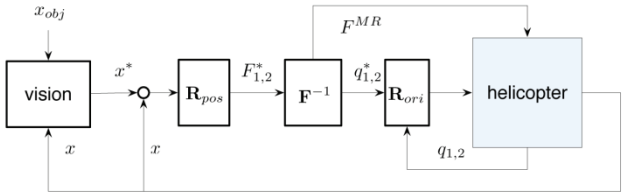

Figure 3. Control scheme used for experimental set-up.

The autonomous manipulation can be decomposed in the following phases:

1. Approaching phase. The helicopter is guided to some position not far from the object. The control system uses the GPS, eventually with the differential corrections (DGPS). If the position of the object is not known, the perception system on board the aerial robot (see Fig. 3) should be able to detect and localize the object. In the ARCAS project, radio systems with a transmitter embedded in the object are also being used.
2. Precise positioning control. In this case the perception system can be used to calculate the position and orientation of the object, and grasping configurations. The output of the vision system was used only to calculate the appropriate desired position of the helicopter (see Fig. 3). The lack of reliability of the perception system in outdoor scenarios should be analysed. In particular, it is well-known that vision systems are significantly affected by environmental problems such as occlusions and variability of lighting conditions. If the pose of the object is known, sensor data fusion with DGPS is very valuable. With ideal weather conditions, we could achieve a precision of TCP positioning up to 1 cm.
3. Manipulation control. This phase refers to the control of the helicopter and manipulator in the last phase. This can be realized using one of the following approaches or their combinations:

a) Completely decoupled control. The helicopter and the manipulator are controlled independently. Usually, the helicopter will try to maintain a hovering position trying to compensate the disturbances from the manipulator; the manipulator

will try to keep the TCP on the object compensating the disturbances caused by the helicopter movement around the hovering position.

b) Coupling on the kinematical level. The controller for helicopter and manipulator are coupled by the positions and velocities of both subsystems.

c) Coupling on the dynamical level. The overall controller for both subsystems considers the dynamical model of the whole system. This is the most general case and potentially will provide the best possible performance from the theoretical point of view. However, the practical considerations make this general conclusion not obvious. For instance, the quality of the sensor signals, often, does not allow precise state estimation of the coupled system. In addition, the dynamical model of the coupled system is complicated and the model-based controller will usually be sensitive to system parameters, non-modelled effects and disturbances.

When the masses of the helicopter are significantly greater than the mass of the manipulator, the dynamical coupling cannot improve the performance of the whole system significantly and it might be preferable to adopt approaches (a) and (b) for control. However, if the mass of the arm is relatively significant, then the approach (c) to control the force interaction is preferable.

Regardless of which control approach and which system set-up is chosen, the following aspects should be investigated in order to design a particular control scheme and to estimate the achievable control performance:

- precision control of the helicopter
- force interaction between helicopter and environment
- movement of the centre of gravity (CoG) due to the manipulator movement

The understanding of the above listed aspects constitutes a base for further development of approaches and technologies for aerial manipulation.

4. Closed-loop behaviour

A manipulator or other grasping device imposes forces and torques on the helicopter fuselage which influence the helicopter motion. This is illustrated in Fig. 4. The description and analysis of the interaction between helicopter and manipulator is complicated. The translational movement of the helicopter generates the interaction forces between manipulator and the fuselage. These forces change the orientation of the fuselage and the main rotor plane which again results in changes of the translational movement. Please note that the dynamical equations for translation and orientation of the helicopter without manipulator are coupled only in one direction. This means that the equations for the rotation are independent from translational movement, e.g., see eqs. (1). The translation depends, of course, on the orientation of the main rotor plane. For the system composed of a helicopter with a manipulator, there is coupling between translational and rotational dynamics in both directions. The equations of the rotational dynamic depend on the translational movement. This fact makes the analysis of the system and, therefore, the model-based controller design, complicated.

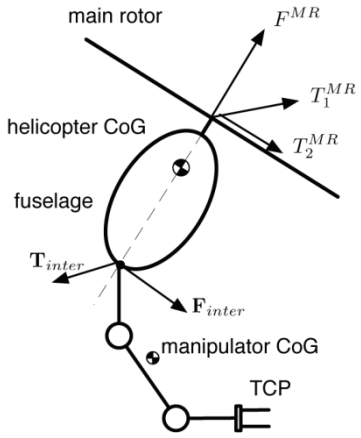

Figure 4. Force torque interaction between manipulator and helicopter fuselage.

4.1 Orientation Controller

The control system is based in the same approach used by the authors for the load transportation system by means of autonomous helicopters. The key element is the orientation controller in the inner loop. The rotation dynamics for a single helicopter, represented by two rigid bodies for the fuselage and the main rotor, can be expressed (see Kondak et al. (2006)) by the following equations:

$$\begin{aligned} T_1^{MR} + K_{12}u_2 + K_{11}\dot{u}_1 = 0 \\ T_2^{MR} + K_{21}u_1 + K_{22}\dot{u}_2 = 0 \end{aligned} \quad (1)$$

where $u_{1,2}$ are rotation speeds of the fuselage, $T_{1,2}^{MR}$ are the torques generated around the longitudinal and lateral axes of the fuselage, and the coefficients K_{xx} are constant parameters of the helicopter and of the main rotor speed. Notice that the rotation speeds couple eqs. (1). This coupling leads to oscillations once the system has been stimulated. Fig. 5 shows the scheme for the control of the helicopter roll and pitch angles $q_{1,2}$. The helicopter controller has the internal control loop with the block $\mathbf{Q}^{-1}$ and the gains K_u for rotation speeds $u_{1,2}$, and the external control loop with the block $\mathbf{D}$ and the gains K_q for the orientation angles $q_{1,2}$. This block $\mathbf{D}$ is used to decouple the plant between $T_{1,2}^{MR}$ and $u_{1,2}$. The block $\mathbf{W}$

in Fig. 5 represents the rotational dynamics described by eqs. (1). The resulting orientation controller shows a good performance and robustness in simulation and real flight experiments with different types of helicopters as it has been shown in Bernard & Kondak (2009); Bernard et al. (2011) ; Kondak et al. (2007); Maza et al. (2010).

Block $\mathbf{D}$ in Fig. 5 only accounts for the rotational dynamic of the manipulator without an arm. In order to consider the motion of the manipulator, this block should be replaced by the inverse rotational dynamics $\tilde{\mathbf{D}}$ not of a single helicopter, but of the whole system (considering both the rotation and translation of each system component).

The simulation experiments have shown that, unlike in the case of a helicopter without a manipulator, the orientation controller with inversion block $\tilde{\mathbf{D}}$ is quite sensitive to variation of the system parameters (5% variation could be critical). To overcome this problem, the use of a force/torque sensor between the manipulator and fuselage is proposed. The measured force $\mathbf{F}_{inter}$ and torque $\mathbf{T}_{inter}$, and the dashed block $\mathbf{C}$ in Fig. 5 are used to calculate the influence on the rotational dynamics of the helicopter from the manipulator and environment. This influence is expressed by means of torque $\mathbf{T}_r = \mathbf{F}_{inter} \times \mathbf{p}_{m-cm} + \mathbf{T}_{inter}$, where $\mathbf{p}_{m-cm}$ is the position vector connecting sensor attaching point m and CoG of the system. The resulting orientation controller is composed of the orientation controller for a helicopter without manipulator and the block $\mathbf{C}$, where $\mathbf{T}_r$ is calculated and subtracted from torques calculated in $\mathbf{D}$."

With the usage of block $\mathbf{C}$, the orientation controller closed-loop system becomes quite simple and very robust against variation of system parameters and disturbances. There are two reasons for this robustness: first, the actual influence of the manipulator on the fuselage is measured through $\mathbf{F}_{inter}$, $\mathbf{T}_{inter}$ and, therefore, the compensation becomes independent from the parameters and state of the manipulator. Second, as long as the orientation of the helicopter is known, the calculated compensation torque is always in the correct phase.

We distinguish between two types of influences imposed on the helicopter from a manipulator: coherent and non-coherent. In case of coherent influence, the forces and torques imposed on the helicopter by the manipulator change with frequencies close to those of the helicopter movement, whereby in the case of non-coherent influence they do not change in time significantly or change with frequencies different to those of the helicopter movement.

The small-size helicopters are insensitive to the non-coherent influences. This can be verified in simulation or by analysis of the dynamical equations as well as in flight experiments. Even large non-coherent torques imposed on the fuselage are compensated by the proposed controller with compensator $\mathbf{C}$.

The opposite is true for the coherent influence. Even small interaction forces imposed on the fuselage periodically in proper phase could yield to low frequency instabilities and oscillations, so-called phase circles. Unfortunately, these phase circles appear often when the manipulator is compensating the helicopter movement in hovering, as explained in Sect. 4.2 in more detail. In this case, the proposed controller with compensator $\mathbf{C}$ works only with a perfectly modelled system. Therefore, for practical applications, in addition to this controller, a coupling between the helicopter and manipulator controllers should be used in order to prevent phase circles.

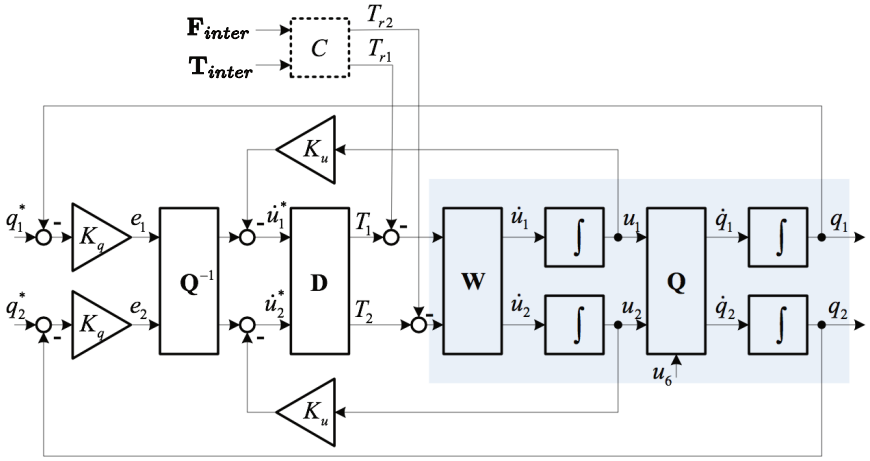

Figure 5. Scheme for the orientation control.

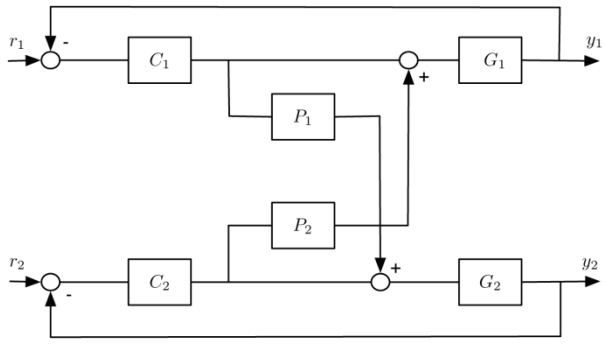

Figure 6. Scheme of the system with a coupling between two outputs y_1 and y_2.

4.2 Movement of the CoG

Let us consider two feedback controlled systems S_1 and S_2 with plants G_1, G_2 and controllers C_1, C_2, as shown in Fig. 6. These feedback systems can correspond to two separate physical systems or be two parts of one physical system. For example, a helicopter with position control allowing an independent motion in $x-$ and $y-$ directions can be considered as composed of two systems with $y_1 = x$ and $y_2 = y$. Often, especially in the case where S_1 and S_2 belong to one physical system, there is a coupling between these two systems, as denoted in Fig. 6 with blocks P_1 and P_2. This undesirable coupling can be caused by model parameter uncertainties, systematic errors in the sensors or by non-modelled physical interconnections between systems S_1 and S_2. This coupling can lead to periodic or coherent energy flow into the systems and induce low frequency oscillations in S_1 and S_2. We demonstrate this for the linear case. Let us consider the transfer function $G_{11} = y_1 / r_1$ for the coupled systems in Fig. 6. It can be shown that

$$G_{11} = \frac{T}{1+T}$$

with

$$T = G_1C_1 - G_1C_2P_2\frac{G_2C_1P_1}{1+G_2C_2}$$

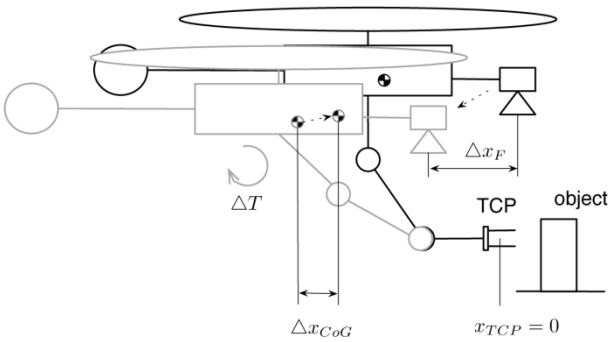

Figure 7. Movement of the manipulator CoG while compensating the displacement of the helicopter.

Considering symmetric systems with $G_1 = G_2 = G, C_1 = C_2 = C$

$$G_{11} = \frac{GC(1+GC(1-P_1P_2))}{1+2GC+G^2C^2(1-P_1P_2)}, \tag{2}$$

where only the product of both coupling blocks P_1P_2 has influence on the system behaviour.

On the other hand, let us consider the set-up for aerial manipulation shown in Fig. 1. Let us imagine that the TCP is fixed on the object (does not move relative to the ground) and the manipulator is compensating the movement of the helicopter caused by a wind gust or the ground effect, see Fig. 7. The displacement of the fuselage $\triangle x_F$ is compensated by the manipulator fixing the TCP at the same position $x_{TCP} = 0$. The resulting displacement of the manipulator CoG $\triangle x_{CoG}$ causes additional torque on the helicopter fuselage $\triangle T$. This additional torque changes the orientation of the helicopter, which yields to some further displacement of the fuselage $\triangle y_F$. The particular issue of a small-size helicopter with a single main rotor is that the torque applied to the fuselage yields the displacement in the same axis as a torque vector or, in our example, perpendicular to the direction of $\triangle x_F$. The fact that $\triangle y_F \perp \triangle x_F$ is important because this is the reason for the existence of low frequency diverging oscillations, i.e., phase circles (as it will be shown later).

To see that $\triangle y_F \perp \triangle x_F$, it is considered the solution of the eqs. (1) for constant input torques T_1^{MR} and T_2^{MR} which is given by

$$\begin{aligned} u_1(t) &= -\frac{T_2^{MR}}{2\beta} + [C_1\cos(\tilde{\alpha}t) - C_2\sin(\tilde{\alpha}t)] \\ u_2(t) &= \frac{T_1^{MR}}{2\beta} + \left[C_2\cos\left(\tilde{\alpha}t\right) + C_1\sin\left(\tilde{\alpha}t\right)\right] \end{aligned} \tag{3}$$

Here β depends on the rotor properties and its rotation speed around the rotor axis (which is assumed to be constant). Furthermore

$$\tilde{\alpha} = 2\omega_{MR}\gamma$$

where γ is a function of mass and geometry properties of the fuselage and the rotor, and ω_{MR} is the rotation speed of the rotor. Depending on the particular system, or its value of γ, the oscillations in eqs. (3) can be neglected or taken into account. In any case the first part

$$\begin{aligned} u_1 &= -\frac{T_2^{MR}}{2\beta} \\ u_2 &= \frac{T_1^{MR}}{2\beta} \end{aligned} \tag{4}$$

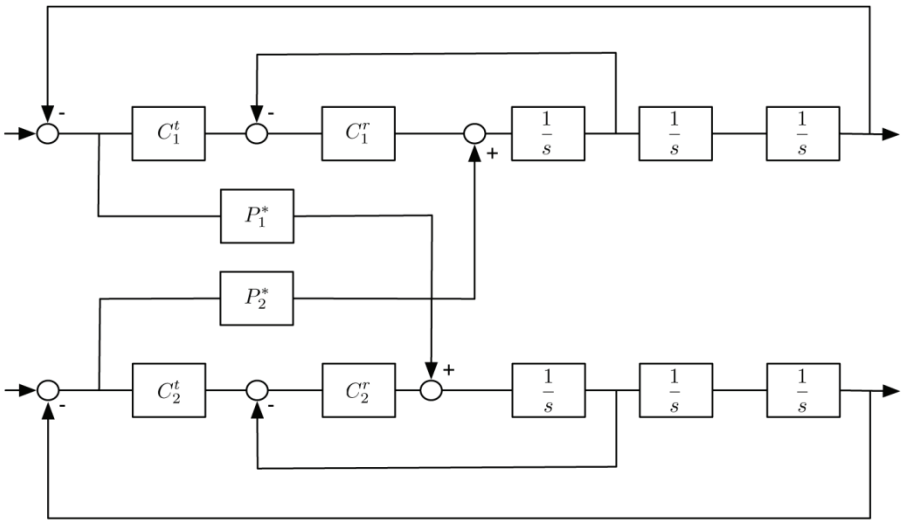

Figure 8. Simplified scheme of the helicopter with manipulator using decoupled control.

shows that, due to the gyroscopic effect of the main rotor, the applied torque induces the rotation speed of the fuselage in perpendicular direction, e.g., $T_2^{MR} \rightarrow u_1$, and the corresponding change in the orientation generates an additional component of the lifting force or acceleration a_2 which is perpendicular to the axis of u_1. Therefore, the complete chain in our example is the following:

$$\Delta x_F \rightarrow \Delta T_2 \rightarrow u_1 \rightarrow q_1 \rightarrow a_2 \rightarrow \Delta y_F \tag{5}$$

where coordinates x, y corresponds to axes 1, 2 and q_1 is the orientation angle around axis 1.

Taking into account that $\Delta y_F \perp \Delta x_F$ and the chain (5), the interaction between the helicopter and manipulator by fixing TCP relative to some object in the environment could be described by the scheme shown in Fig. 8. Without the blocks P_1^* and P_2^*, this scheme represents the motion of a controlled helicopter along $x-$ and $y-$axis. Here a simplified form for rotational dynamics represented by one integrator is used. $C_{1,2}^r$ are orientation controllers and $C_{1,2}^t$ are translation controllers for axes 1, 2. Using this scheme, the existence of phase circles in this case will be investigated.

It can be shown that the transfer function $G_{11} = y_1 / r_1 G_{11}$, eq. (2) in the case of a symmetric system with $C_1^{r,t} = C_2^{r,t}$ is

$$G_{11} = \frac{C^r C^t s^3 + (C^r)^2 C^{tr} s^2 + (C^r C^t)^2 - P_1^* P_2^*}{s^6 + 2C^r s^5 + (C^r) s^4 + 2(C^r C^t)^2 s^3 + 2(C^r)^2 C^t s^2 + (C^r C^t)^2 - P_1^* P_2^*}$$

Using for $C^r = K_q$, for $C^t = K_d s + K_p$ with $K_q = 3, K_d = 2, K_p = 1$, the following G_{11} transfer function is obtained

$$G_{11} = \frac{3(3 + 12s + 15s^2 + 7s^3 + 2s^4) - P_1^* P_2^*}{(3 + 6s + 3s^2 + s^3)^2 - P_1^* P_2^*}$$

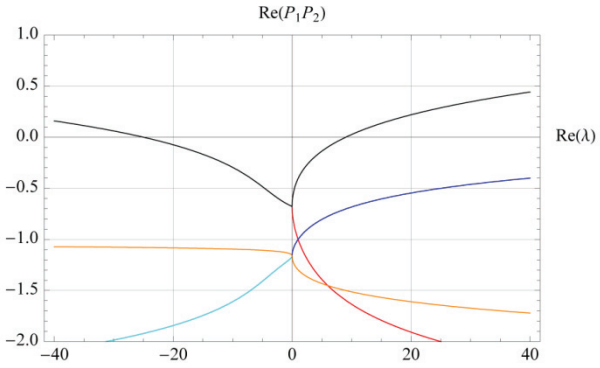

Figure 9. Movement of system poles λ while increasing gains in P_1P_2.

As in (2) $P_1^* P_2^*$ has an influence on the system poles. In Fig. 9, the pole movement for the gain of $P_1\, P_2$, changing in interval [−40; 40], is shown. As it can be seen in points $Re\ (P_1^* P_2^*) = -25$ and $Re(P_1^*\, P_2^*) = 9$, one of the system poles' real part gets positive (or moves to the right half of the s-plain). This means that the system starts to move on the phase circles. In Fig. 10, an example of such movement is shown. The different sign of the two points $Re\ (P_1^* P_2^*) = -25$ and $Re(P_1^*\, P_2^*) = 9$ means that phase circles can appear for P_1^* and P_2^* with the same, as well as a different, sign.

One possible solution to avoid phase circles is to set P_1^* or P_2^* to zero. In our case this can be done by restricting the motion of manipulator CoG by setting

$$\Delta y_{CoG} = 0 \tag{6}$$

This means that manipulator CoG moves only in $xz-$ plain, so $P_2^* = 0$ and the phase circles cannot appear for any set of system parameters. The condition (6) can be realized e.g. using a manipulator with 7 DoF.

In Fig. 10, the two horizontal coordinates (x, y) of a helicopter moving in a simulation experiment are shown. In this experiment, the TCP position is fixed in an inertial frame and the manipulator compensates the movement of the helicopter. The helicopter and the manipulator are controlled independently and condition (6) is not satisfied. As it can be seen, the phase circles appear and the helicopter controller is not able to stabilize its hovering configuration. In Fig. 11, the motion of the same system in simulation is shown. Different to the previous case, here condition (6) is satisfied, and the manipulator CoG is moving only along the $x-$axis. We can see that the helicopter controller stabilizes the hovering configuration and the phase circles do not appear.

Please note that even if the displacement of the manipulator CoG and the corresponding torques acting on the fuselage are small, compared to torques generated by the main rotor, they act in the phase with the fuselage movement and can induce phase circles. The disturbance torque, imposed on the fuselage, which is not changing in the phase with the fuselage movement, e.g., static displacement of the CoG, does not cause the phase circles described above and can be rejected by the helicopter controller well - even if its absolute value is comparable with the torques generated by the main rotor.

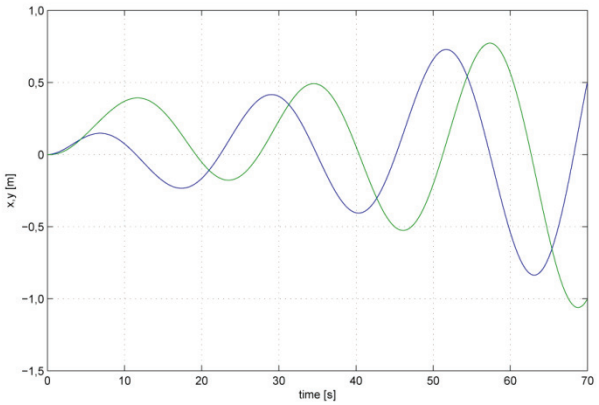

Figure 10. Movement of the helicopter induced by a manipulator which moves its CoG in two dimensions (horizontal plain).

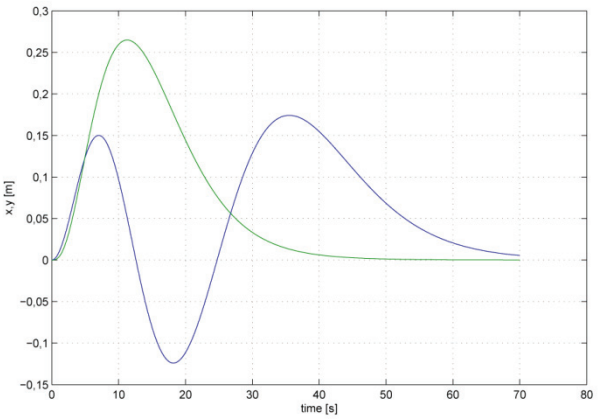

Figure 11. Movement of the helicopter induced by a manipulator which moves its CoG along only one dimension.

Figure 12. Experimental platform with pendulum for displacement of the helicopter CoG.

Condition (6) and the results from the second simulation experiment shown in Fig. 11 are verified in flight experiments using the set-up shown in Fig. 12. An electrical helicopter with the take-off weight of 15 kg is equipped with a pendulum, which can move a mass of 1 kg along the roll axis of the fuselage. The distance between the pendulum CoG and its rotation point is 0.12 m. The displacement of the pendulum CoG, while hovering, did not induce the oscillations as shown in Fig. 10.

5. Conclusions

Aerial robots physically interacting with the environment could be very useful for many applications. However, the models involved in the design of the control system are complicated due to dynamic coupling between the parts of the system. This was illustrated in the particular case of autonomous helicopters used for aerial manipulation. It was also shown that for analysis and control design of helicopters with manipulators, simplifications could be found which lead to practical, relevant solutions. Preliminary results for aerial manipulation were presented and discussed. In particular, it has been shown that if the forces and torques imposed by a manipulator on a helicopter change with frequencies close to those of the helicopter movement, even small interaction forces can generate low frequency instabilities and oscillations, so-called phase circles.

6. Acknowledgements

This work was partially supported by the projects ARCAS (European Commission, 7 th Framework Program, ICT-2011-287617) and by the national projects RANCOM (P11-TIC-7066) and CLEAR (DPI2011-28937-C02-01).

7. References

[1] Albers, A., Trautmann, S., Howard, T., Nguyen, T. A., Frietsch, M. & Sauter, C. (2010). Semiautonomous flying robot for physical interaction with environment, *Robotics, Automation and Mechatronics*.

[2] Bernard, M. & Kondak, K. (2009). Generic slung load transportation system using small size helicopters., *ICRA*, IEEE, pp. 3258–3264. URL: *http://dx.doi.org/10.1109/ROBOT.2009.5152382*

[3] Bernard, M., Kondak, K., Maza, I. & Ollero, A. (2011). Autonomous transportation and deployment with aerial robots for search and rescue missions, *Journal of Field Robotics* 28(6): 914–931. URL: *http://dx.doi.org/10.1002/rob.20401*

[4] Caccavale, F. & Siciliano, B. (2001). Kinematic control of redundant free-floating robotic systems, *Advanced Robotics* 15(4): 429–448. URL: *http://www.tandfonline.com/doi/abs/10.1163/156855301750398347*

[5] Kondak, K., Bernard, M., Losse, N. & Hommel, G. (2006). Elaborated modeling and control for autonomous small size helicopters, *International ISR/Robotik Joint Conference*, VDI, pp. 207–208.

[6] Kondak, K., Bernard, M., Meyer, N. & Hommel, G. (2007). Autonomously flying VTOL-robots: Modeling and control, *ICRA*, IEEE, pp. 736–741. URL: *http://dx.doi.org/10.1109/ROBOT.2007.363074*

[7] Korpela, C. M., Danko, T. W. & Oh, P. Y. (2012). MM-UAV: Mobile manipulating unmanned aerial vehicle, *Journal of Intelligent and Robotic Systems* 65(1-4): 93–101. URL: *http://dx.doi.org/10.1007/s10846-011-9591-3*

[8] Lindsey, Q., Mellinger, D. & Kumar, V. (2011). Construction of cubic structures with quadrotor teams, *Proceedings of Robotics: Science and Systems*, Los Angeles, CA, USA.

[9] Maza, I., Kondak, K., Bernard, M. & Ollero, A. (2010). Multi-UAV cooperation and control for load transportation and deployment, *Journal of Intelligent and Robotic Systems* 57(1–4): 417–449.

[10] Mellinger, D., Lindsey, Q., Shomin, M. & Kumar, V. (2011). Design, modeling, estimation and control for aerial grasping and manipulation, *IROS*, IEEE, pp. 2668–2673. URL: *http://dx.doi.org/10.1109/IROS.2011.6094871*

[11] Mellinger, D., Shomin, M., Michael, N. & Kumar, V. (2010). Cooperative grasping and transport using multiple quadrotors, *Proceedings of the International Symposium on Distributed Autonomous Robotic Systems*.

[12] Moosavian, S. A. A. & Papadopoulos, E. (1998). On the kinematics of multiple manipulator space free-flyers and their computation, *Journal of Robotic Systems* 15(4): 207–216. URL: *http://dx.doi.org/10.1002/(SICI)1097-4563(199804)15:4<207::AID-ROB3>3.0.CO;2-T*

[13] Moosavian, S. A. A. & Papadopoulos, E. (2007). Free-flying robots in space: an overview of dynamics modeling, planning and control, *Robotica* 25(5): 537–547. URL: *http://dx.doi.org/10.1017/S0263574707003438*

[14] Orsag, M., Korpela, C. & Oh, P. (2012). Modeling and control of MM-UAV: Mobile manipulating unmanned aerial vehicle, *Proc. of the International Conference on Unmanned Aircraft Systems*.

[15] Pounds, P. & Dollar, A. (2010). Hovering stability of helicopters with elastic constraints, *Proceedings of the ASME Dynamic Systems and Control Conference*.

[16] Pounds, P. E. I., Bersak, D. R. & Dollar, A. M. (2011). Grasping from the air: Hovering capture and load stability, *ICRA*, IEEE, pp. 2491–2498. URL: *http://dx.doi.org/10.1109/ICRA.2011.5980314*

[17] Umetani, Y. & Yoshida, K. (1987). Continuous path control of space manipulators mounted on OMV, *Acta Astronautica* 15(12): 981 – 986. URL: *http://www.sciencedirect.com/science/article/pii/0094576587900221*

[18] Vafa, Z. & Dubowsky, S. (1987). On the dynamics of manipulators in space using the virtual manipulator approach, *ICRA*, Vol. 4, pp. 579 – 585.

[19] Vafa, Z. & Dubowsky, S. (1990). The kinematics and dynamics of space manipulators: the virtual manipulator approach, *International Journal of Robotics Research* 9(4): 3–21. URL: *http://dx.doi.org/10.1177/027836499000900401*